Title	Enhanced soft magnetic properties in N-doped amorphous FeCo thin film
Authors	Das, Rajasree;Wei, Guan-Nan;Lordan, Daniel;Hayes, Mike;Clarke, Barry;Hurley, David;Ó Mathúna, Cian;Sai, Ranajit;McCloskey, Paul
Publication date	2023-06-26
Original Citation	Das, R., Wei, G.-N., Lordan, D., Hayes, M., Clarke, B., Hurley, D., Ó Mathúna, C., Sai, R. and McCloskey, P. (2023) 'Enhanced soft magnetic properties in N-doped amorphous FeCo thin film', IEEE Transactions on Magnetics, 59(11), 2001305 (5pp). doi: 10.1109/TMAG.2023.3287682
Type of publication	Article (peer-reviewed)
Link to publisher's version	10.1109/tmag.2023.3287682
Rights	© 2023, IEEE. Personal use of this material is permitted. Permission from IEEE must be obtained for all other uses, in any current or future media, including reprinting/republishing this material for advertising or promotional purposes, creating new collective works, for resale or redistribution to servers or lists, or reuse of any copyrighted component of this work in other works.
Download date	2025-01-13 21:29:23
Item downloaded from	https://hdl.handle.net/10468/14928

This article has been accepted for publication in IEEE Transactions on Magnetics. This is the author's version which has not been fully edited and content may change prior to final publication. Citation information: DOI 10.1109/TMAG.2023.3287682

Enhanced soft magnetic properties in N-doped amorphous FeCo thin film

Rajasree Das[1,*], Guan-Nan Wei[1], Daniel Lordan[1], Mike Hayes[1,2], Barry Clarke[3], David Hurley[3], Cian. Ó. Mathúna[1], Ranajit Sai[1] and Paul McCloskey[1]

[1]Microsystems Centre, Tyndall National Institute, University College Cork, Cork, Ireland, rajasree.das@tyndall.ie
[2]ICT for Energy Efficiency, Tyndall National Institute, University College Cork, Cork, Ireland
[3] TEL Magnetic Solutions Ltd (TELMS), Dublin 9, Ireland

Sputtered $FeCoN_x$ thin films with various nitrogen fraction are investigated in the quest of low lossy, soft magnetic thin films (SMFs) for high frequency inductor core. 100-nm thick $FeCoN_x$ films were deposited in N_2+Ar environment (5 mTorr) with increasing N_2 volume percent, $x\% = N_2/(Ar + N_2)$, up to 30%. While FeCo thin film is isotropic, incorporation of nitrogen in the film exhibits a well-defined uniaxial magnetic anisotropy (UMA) as a result of reduced stress in the $FeCoN_x$ films. $FeCoN_{17.5}$ thin film with UMA shows superior all-round soft magnetic properties (saturation flux density ~ 1.7 T, coercivity ~ 7.8 Oe, real permeability ~ 381.7 and resistivity ~ 201 µΩ.cm). Study of the dynamic magnetic properties of $FeCoN_x$ (x= 15, 17.5 and 19%) films reveal two ferromagnetic resonance (FMR) peaks. Double resonance peaks in films with high concentration of nitrogen might be related to FeCo and Fe-N multiphase in the films. Furthermore, evolution of the real (μ') and imaginary (μ'') part of the permeability spectra in the presence of dc magnetic bias field is also examined.

***Index Terms*— Soft magnetic thin films, magnetic anisotropy, FeCo magnetic materials, permeability, saturation flux density.**

I. Introduction

FUTURE electronic devices demand efficient and miniaturized power delivery subsystems, such as dc-dc converters. The main obstacle towards miniaturization of the converters is the volume and weight of their passive components, i.e, transformers and/or inductors. Increasing the application switching frequency facilitates system integration towards Power System on Chip (PwrSoC) [1]. However, high switching frequencies entail enhanced core loss that eventually reduces the power conversion efficiency. Therefore, fabrication of integrated passive components of small size and high efficiency requires magnetic cores featuring high magnetic flux density to handle large current, low coercivity to stem hysteresis loss, and high electrical resistivity to reduce eddy-current losses. Significant progresses have been made in identifying suitable soft magnetic material integration technology, designs and material research [2]–[5].

Amorphous ferromagnetic alloys like CoZrTa, CoZrNb, NiFe boast with significantly higher saturation flux density B_s (~1.2-1.4 T) than ferrites (~0.5 T) but possess very low resistivity, ρ (~100 µΩ-cm) [6], [7]. Such a low resistivity entails significant eddy current losses in the magnetic materials at the frequency of interests (~100 MHz) for integrated voltage regulator (IVRs) applications [4]. On the other hand, owing to their high B_s (>2 T), Fe-based amorphous alloys like FeCoB, FeCo, FeC, etc. are gaining popularity in recent years [8], [9]. However, prohibitively large coercivity and low-resistivity in them remains an issue.

Among all these compositions, nitrides of FeCo thin films displayed the glimpses of all the right qualities (high B_s, low H_c, high anisotropy, and high value of ρ) required for high-frequency applications [10]–[12]. Magnetic properties (static and dynamic) of FeCo-nitride films are hugely affected by slight variation in the microstructure, opening lot of opportunities to alter their properties according to the requirement of the application. To mention a few, high efficiency transformers and inductors require a high value of the real part of permeability, whereas, electromagnetic wave attenuators require high imaginary permeability as well [13].

The magnetic flux density of $Fe_{1-x}Co_x$ ($0.3 < x < 0.5$) is very high ~2.4 T [10], however, in-plane anisotropy and low coercivity is difficult to achieve in these films due to high magnetostriction constant (λ_S= 45-65 x 10^{-6}). Jung *et. al.* [14] reported a drastic decrease of H_c from 120 Oe to 1-3 Oe (along hard axis) in $Fe_{0.65}Co_{0.35}$ films deposited on various under layers (Cu, NiFe, and Ru). Similarly, introducing nitrogen has also proven to be very effective to deposit high resistive film with soft magnetic properties [10], [15], [16]. However, high B_s and low H_c can be obtained only at an optimized value of nitrogen concentration, as at high concentration the magnetic properties are adversely affected. An extensive study on the effect of nitrogen concentration and substrate temperature by Kuo *et. al.* shows B_s of 2.39T for $(Fe_{0.9}Co_{0.1})_{0.92}N_{0.08}$ thin film deposited at substrate temperature near 200 °C, however, H_c was high (~80 Oe) [15]. Later, very low H_c of 0.6 Oe and B_s of 2.4 T are reported for a sandwiched structure of $Ni_{0.81}Fe_{0.19}/(Fe_{0.7}Co_{0.3})_{0.95}N_{0.05}/Ni_{0.81}Fe_{0.19}$ [10]. Although desired B_s and H_c are achieved in the sandwich structure, resistivity (~50 µΩ.cm) of the laminated film was poorer than CoZrTa due to incorporation of permalloy.

Here we report fabrication and physical properties of single layer soft magnetic films (SMFs), $FeCoN_x$, with high saturation flux density, high resistivity, and pronounced magnetic anisotropy without any under layer. Having magnetic anisotropy is necessary to reduce core loss further by limiting the core switching to magnetic hard axis switching [17].

II. EXPERIMENTAL

Nitrogen incorporated FeCo-SMFs with 100 nm thickness were deposited on Si (100) substrates, with 250 nm thermally grown SiO_2 top layer, using a dc magnetron sputtering system (Kurt J. Lesker Sputterer CMS-18). High purity (~99.99%) $Fe_{65}Co_{35}$ targets were used for all the depositions. Base pressure of the chamber prior to all the depositions was maintained below 1 x 10^{-7} Torr, whereas, during depositions Ar + N_2 pressure was maintained at 5 mTorr. Films were grown at various N_2 concentrations by varying N_2 volume percent, $x\% = N_2/(Ar + N_2)$, between 0 and 30% in the chamber. Total 9 compositions of nitrogen incorporated FeCo films were prepared for $x\%$ = 0, 5, 10, 12.5, 15, 17.5, 19, 20 and 30 and the corresponding films are named as FeCo, $FeCoN_5$, $FeCoN_{10}$ and so on, respectively.

KLA-Tencor P-17 Profiler was used to calibrate deposition rate and later to obtain stress and thickness of each film. To obtain the stress generated precisely due to the sputtered film, stress of the 4-inch wafer was measured before and after every film depositions, using the profiler for scan length of 80 mm. Pre and post-film stress profile and the magnetic film thickness were provided as input to calculate the film stress. Surface morphology and magnetic images were taken with an AFM (Bruker Dimension Icon). Structure of the films was examined by powder x-ray diffractometer (XRD, Philips X'pert diffractometer, Cu-K_α radiation with λ=1.54 Å). Room temperature resistivity was measured using a 4-point probe setup. The dc magnetic properties of 4-inch wafers were investigated by using a B-H loop tracer (SHB, MESA 200 HF). Magnetic field dependent magnetization was measured while the dc field was applied parallel to sample plane and the wafer was rotated in-plane to obtain both the easy and hard magnetic direction of the deposited film. Real and imaginary part of the permeability of all the films were measured using a high-frequency Permeameter (Ryowa, PMM 9G) at room temperature.

TABLE I: Properties of FeCo and $FeCoN_x$ films (at different N_2 volume percent, x).

Properties	$FeCoN_x$ (x in %)			
	$x = 0$	15	17.5	19
Stress (GPa)	1.1	0.85	0.89	0.74
Resistivity (μΩ.cm)	35	184	201	244
rms roughness (nm)	0.17	1.7	1.8	1.6
Saturation flux density, B_s (T)	2.5	2.1	1.7	1.4
Coercivity, H_c (Oe) (along hard axis)	100	16	7.8	9.3
Anisotropy field, H_k (Oe)	-	62	63	65
Relative permeability,μ (at 100 MHz)	10	192.4	381.7	187.2

III. RESULTS AND DISCUSSION

A. Topology and structure

Atomic force microscopy (AFM) images show the surface morphology of FeCo and $FeCoN_{17.5}$ films as presented in Fig. 1(a). Nitrogen incorporation enhances grain size in the films and an indication of nanocluster formation is observed in $FeCoN_{17.5}$. Root means square roughness measurement over 10 μm x 10 μm scan shows relatively smooth surfaces for both FeCo and $FeCoN_{17.5}$ (0.17 nm and 1.80 nm, respectively). However, films grown in nitrogen environment show very different microscopic features (nanoclusters and higher rms roughness), which influences resistivity of the films.

Fig. 1(b-c) illustrates XRD pattern of $FeCoN_x$ films (x = 0, 15, 17.5 and 19), deposited at different N_2 volume percent. XRD of sputtered FeCo film measured at ambient temperature shows (Fig. 1b) strong background signal at low 2θ values – indicative of an amorphous matrix. In addition, a nanocrystalline peak (Fig. 1b inset) that appears at 2θ= 44.9° can be indexed as BCC α-FeCo (110) phase [18]. Other intense peaks are originated from the Si/SiO_2 substrate. Therefore, it can be summarized that the deposited film comprised of a tiny quantity of nanocrystalline α-FeCo phase embedded in an amorphous matrix. As the films were deposited in Ar + N_2 atmosphere, nitrogen atoms occupied interstitial sites, causing mixture of FeCo amorphous phases and undetermined quantity of $\alpha', \alpha'', \gamma', \varepsilon$ and ζ phases of FeN in these films [18], [19]. Inset of Fig 1(c) shows $FeCoN_x$ has very small peaks around 2θ= 43.0° - 46.3°. It is very likely that α''-$Fe_{16}N_2$ and γ'-Fe_4N phases appears in $FeCoN_{15}$ and $FeCoN_{17.5}$ films, whereas, $FeCoN_{19}$ has ε-Fe_3N phase. 4-point probe resistivity measurement (Fig. 1(d)) indicates that ρ is enhanced by nearly an order of magnitude in $FeCoN_{19}$ film (TABLE I), which is even higher than the Co–Zr–Ta–B systems [6]. A higher resistivity in soft magnetic thin film is desirable to reduce eddy current losses [7]. ρ is maximum for $FeCoN_{19}$ film and it starts to decay with further enhancement in x (Fig. 1(d)).

Stress of the film remains tensile with a gradual decreased value for the films deposited at higher N_2 volume percent (Fig. 1(c)).

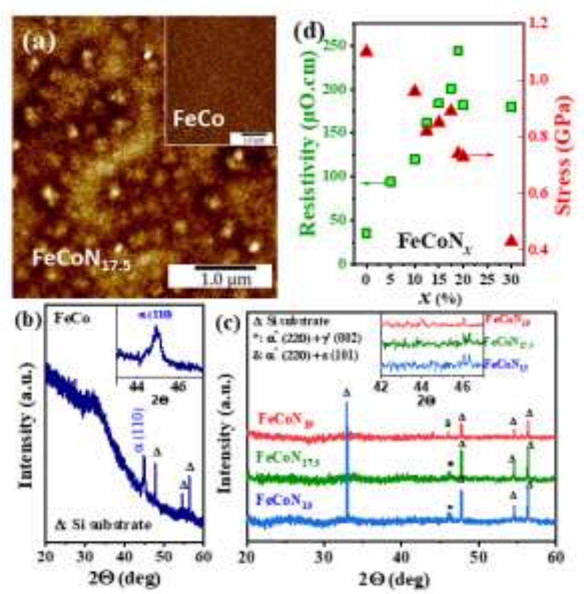

Fig. 1. (color online) (a) AFM images of $FeCoN_{17.5}$ films and the inset shows topology of FeCo film. (b) XRD diffraction pattern of FeCo amorphous film with a nanocrystalline α-FeCo (110) phase and (c) XRD diffraction pattern of $FeCoN_x$ films containing FeCo amorphous phase and possible fractions of α''-$Fe_{16}N_2$ (220), γ'-Fe_4N (002) and ε-Fe_3N (101) phases. (d) Variation in resistivity (left) and stress (right) of $FeCoN_x$ films fabricated at different N_2 volume percent.

This article has been accepted for publication in IEEE Transactions on Magnetics. This is the author's version which has not been fully edited and content may change prior to final publication. Citation information: DOI 10.1109/TMAG.2023.3287682

B. Static and dynamic magnetic studies

In-plane *M-H* hysteresis loop of the $FeCoN_x$ films (100 nm) deposited at different N_2 volume percent, x are shown in Fig 2(a-d). The film deposited without nitrogen atmosphere is found to be isotropic in nature, whereas, introduction of nitrogen in the FeCo film has transformed it to in-plane anisotropic. All $FeCoN_x$ films show different magnetic hysteresis along easy and hard anisotropy axis. H_c decreased dramatically by introducing nitrogen in FeCo during sputtering, i.e. $FeCoN_x$ has much better soft magnetic properties compared to FeCo of the same thickness. Fig 2(c) demonstrates that $FeCoN_{17.5}$ film exhibits in-plane uniaxial magnetic anisotropy (UMA) with moderate anisotropy field, H_k of 63 Oe and low H_c of 7.8 Oe along the magnetic hard axis direction. Magnetic parameters (B_s, H_c and H_k) of few SMFs are tabulated in TABLE I.

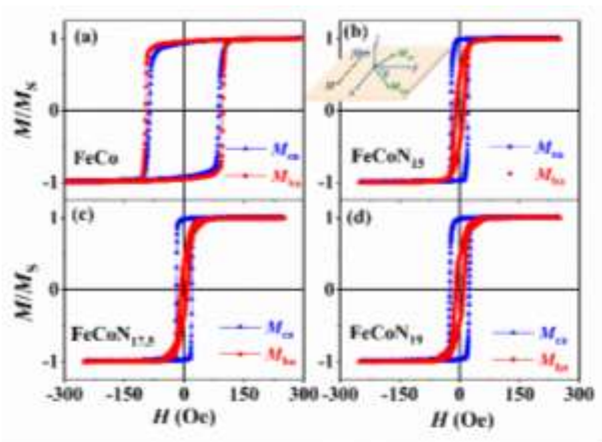

Fig. 2. (color online) Room temperature dc magnetization as a function of applied field (H) for FeCo thin film (100 nm) deposited at different N_2 volume percent. M_{ea} and M_{ha} correspond to the magnetization along easy and hard magnetic axis of the films, respectively.

Fig. 3 indicates modification of B_s and H_c with x in $FeCoN_x$ films. As N_2 volume percent increases from 0 to 12.5%, B_S shows a gradual decrease, but at N_2 of 15% B_s suddenly jumps up to ~2.07 T followed by a decay when B_s drops to 0.4 T for N_2 of 20%. Similarly, H_c initially decreased, showed minima at N_2 of 17.5% and then increases steeply with higher N_2 volume percent. The lowest H_c of ~7.8 Oe is achieved along hard axis in $FeCoN_{17.5}$ which is better than the recently reported FeCo/Au system [9]. It is worth mentioning that as nitrogen was introduced to the films, tensile stress came down to 0.89 GPa in $FeCoN_{17.5}$ from a value of 1.1 GPa in FeCo. Thus, introduction of nitrogen in FeCo system reduces the residual stress, in addition to the alteration in the microstructure and formation of an easy magnetization direction in the film [20]. In addition to these, literature indicates magnetic properties of iron nitride films strongly depend on N_2 volume percent [19], [21]. Several nitride phases $\alpha', \alpha'', \gamma', \varepsilon$ and ζ, with different crystal structures and magnetic properties form in sequence as nitrogen fraction increases. Among these, α''-$Fe_{16}N_2$ phase, forms at comparatively lower N_2 volume percent, where the nitrogen atoms are ordered in the interstitial site, has the maximum magnetic saturation and lowest coercivity. The formation of γ'-Fe_4N and ε-Fe_3N phases, afterwards at higher N_2 volume percent is known to lower the magnetization and raise the coercivity of the magnetic nitride films. This explains the poor soft magnetic properties in $FeCoN_{19}$ folm that deposited at a very high volume percent of N_2. Magnetic softness of these films could be further enhanced by controlling the grain size and optimizing film thicknesses [22]. Sun *et. al*. has reported that proportionality relation between coercivity and grain size isn't valid for FeCo (with 30 at% Co) films, due to their non-negligible magnetoelastic anisotropy (K_σ = -95 mJ/m^3). For thick films (thickness > 100 nm), coercivity is inversely proportional with the mean grain size [22].

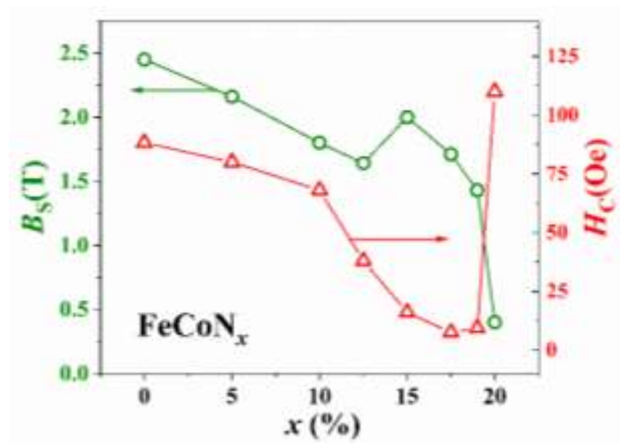

Fig. 3. (color online) The changes of saturation magnetization (B_S) and coercivity (H_C) with nitrogen volume percent for $FeCoN_x$ films.

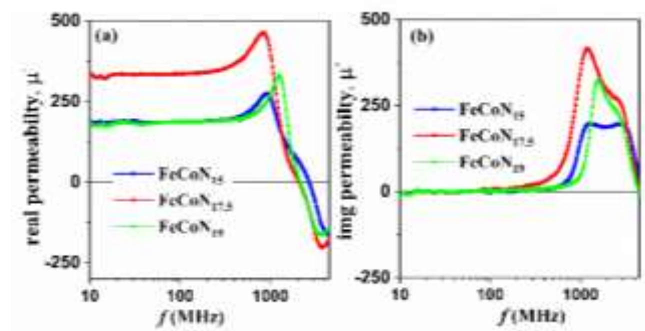

Fig. 4. (color online) High frequency (a) real permeability, μ' and (b) imaginary permeability, μ'' spectra of $FeCoN_x$ films (x= 15, 17.5 and 19) under zero bias field.

In addition to low H_c, $FeCoN_x$ shows an improved ac magnetic response. Frequency dispersion of magnetic permeability, $\mu = \mu' - i\mu''$, of the films are measured at the frequency range 10-4500 MHz (Fig 4). μ' is very sensitive to the nitrogen volume percent in the chamber while depositing the SMFs. $FeCoN_{17.5}$ displays the highest relative permeability of 381.7 at 100 MHz. However, with further increasing the N_2 volume percent to 19%, μ' is reduced (TABLE I). Frequency dependent permeability spectra of the $FeCoN_x$-SMFs shows very distinct double resonance phenomenon and wide magnetic loss spectra with absorption peaks at frequency, f_{r1} ~1.2 GHz and f_{r2} > 2.5 GHz. However, absence of multidomain resonance peak below f_{r1} ensures magnetic homogeneity of the $FeCoN_x$-

This article has been accepted for publication in IEEE Transactions on Magnetics. This is the author's version which has not been fully edited and content may change prior to final publication. Citation information: DOI 10.1109/TMAG.2023.3287682

SMFs [23]. These observations confirm that developing FeCo in nitrogen environment has positive effect on the magnetic properties and it can be further improved by tailoring the thickness of the film [20], [23]. The reason behind two resonance peaks in $FeCoN_x$ films, could be the existence of two magnetic phases, FeCo and some Fe-N phase(s). In $[FeCo/FeCo\text{-}SiO_2]_n$ multilayer films, different dynamic anisotropies for FeCo and $FeCo\text{-}SiO_2$ layers contribute to two resonance peaks in the frequency dependent permeability spectra [24]. However, it is not straightforward to quantify the dispersion of the multiphase dynamic anisotropy fields [24], [25].

The complex permeability spectra of SMF $FeCoN_{17.5}$ with highest permeability value is measured under various external bias field (H_{bias}) to investigate the characteristics of f_{r1} and f_{r2} peaks. As shown in Fig. 5, in the absence of a dc magnetic field, μ' increases slowly with frequency and shows a peak at frequency ~ 0.85 GHz. Application of dc bias field shifts μ' and μ'' peaks toward higher frequency positions till the static magnetic saturation is reached (inset of Fig 5). f_{r1} and f_{r2} move to a higher frequency of ~ 2.5 GHz and ~3.9 GHz, respectively, at 100 Oe bias field (inset of Fig 5(b)). Both μ' and μ'' are strongly suppressed at H_{bias} of 300 Oe.

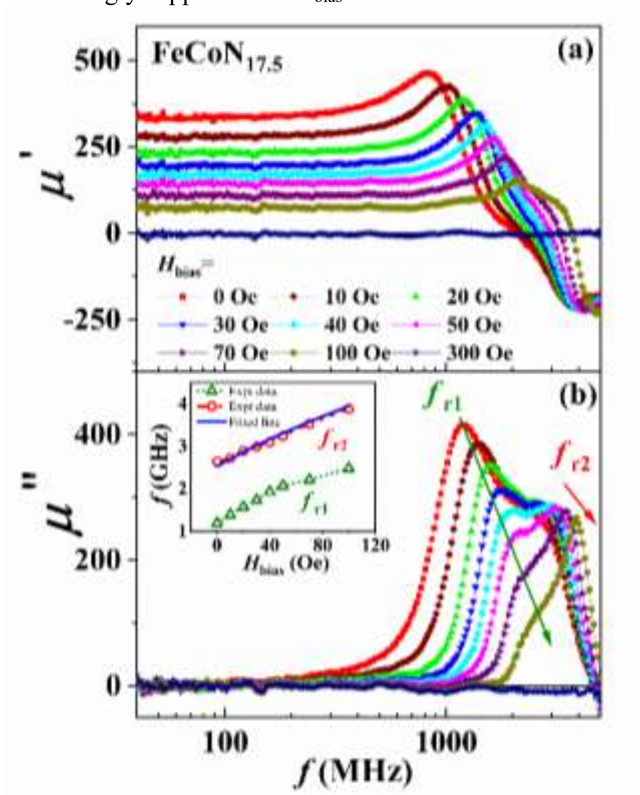

Fig. 5. (color online) (a) Real permeability, μ' and (b) imaginary permeability, μ'' spectra of $FeCoN_{17.5}$ film at various external dc magnetic field (H_{bias}). Inset of (b) shows shift of both resonance peaks (f_{r1} and f_{r2}) with increasing H_{bias}. Symbols present the experimental data and the fitting of f_{r2}-H_{bias} curve with the Kittel's equation is presented by solid line.

The shift of both resonance peaks (f_{r1} and f_{r2}) towards higher frequencies with increasing H_{bias} confirms the ferromagnetic nature of the resonance peaks (Inset of Fig 5(b)) [26]. Monotonic increase of f_{r2} with H_{bias} indicates electron spin type resonance resulting from the main amorphous FeCo phase. In contrast, f_{r1} exhibits a two-step increase of FMR – indicative of the presence of multiple magnetic phases of varied cluster sizes as evidenced in the XRD and AFM data (Fig 1).

Spin resonance frequency shifts towards higher frequency as the external bias field, H_{bias}, is applied. The Kittel condition for the in-plane ferromagnetc resonance (FMR) indicates how the resonance frequency, f_r, changes with the applied bias field, expressed as, $f_r = \frac{\gamma}{2\pi}\sqrt{(H_k + H_{bias})(H_k + 4\pi M_S + H_{bias})}$,[28] where $4\pi M_S$ is the saturation magnetization, and γ the gyromagnetic ratio, is related to the Landé g-factor with the relation $\gamma = (g\mu_B/\hbar)$, where $\hbar$ is the reduced Planck's constant and μ_B is the Bohr magneton. f_{r2}-H_{bias} curve was fitted with the Kittel's equation and γ of 1.45×10^7 $s^{-1}.Oe^{-1}$ and anisotropy field of 70 Oe was obtained for $FeCoN_{17.5}$ film.

C. CONCLUSION

Nitrogen incorporated $FeCoN_x$ films with enhanced soft magnetic properties were developed by sputtering. These films are expected to have lower iron losses than FeCo-films as the hysteresis losses and eddy current losses are substantially lowered by reduced coercivity and increased resistivity respectively. Moreover, very low tanδ even at 100 MHz renders insignificant anomalous losses, making them potential core material for the inductors and transformers of next-gen on-chip power converters. Different nitrogen fraction in the films are obtained by altering the N_2 volume percent while keeping the deposition chamber pressure at 5 mTorr. Nearly seven times enhancement in electrical resistivity (244 μΩ.cm) was achieved in $FeCoN_{19}$ compared to FeCo film. The presence of nitrogen affects the high B_s of FeCo film to some extent, but it reduces the coercivity nearly ten-fold. $FeCoN_{17.5}$ film displays lowest H_c of 7.8 Oe with B_s of 1.7 T. Significantly softer magnetic behaviors in $FeCoN_x$ films compared to FeCo could be attributed to reduction in residual stress in presence of nitrogen atoms. Room temperature permeability results indicate ferromagnetic resonance above 1 GHz for all the films. The resonance loss characteristics of the $FeCoN_x$ films exhibits two peaks at ~1 GHz and ~2.5 GHz – indicative of the presence of multiple magnetic phases. At 100 MHz, $FeCoN_{17.5}$ has permeability of 381.7 – the highest among all samples. Ferromagnetic resonance frequency shifts towards higher frequencies with increasing x. High saturation flux density, permeability, resistivity and also ability to tune the FMR frequency over a wide range makes $FeCoN_x$ very useful for high-frequency inductor core application.

ACKNOWLEDGEMENT

This work was supported by funding from TEL Magnetic Solutions Ltd (TELMS) and the Enterprise Ireland - "Innovation Partnership Programme", Contract No: IP 2020 0912

REFERENCES

[1] C. Ó. Mathúna, N. Wang, S. Kulkarni, and S. Roy, "Review of Integrated Magnetics for Power Supply on Chip (PwrSoC)," *IEEE Trans. Power Electron.*, vol. 27, no. 11, pp. 4799–4816, 2012, doi: 10.1109/TPEL.2012.2198891.

[2] D. Dinulovic, L. Haase, M. Haug, and J. Wolf, "Power Microtransformer on Silicon Embedded into PCB," *2021 3rd Int. Symp. 3D Power Electron. Integr. Manuf. 3D-PEIM 2021*, pp. 21–24, 2021, doi: 10.1109/3D-PEIM49630.2021.9497259.

[3] D. Dinulovic, M. Shousha, and M. Haug, "Tiny wafer level chip scale packaged inductive components for high frequency isolated/non-isolated DC-DC converters," *Conf. Proc. - IEEE Appl. Power Electron. Conf. Expo. - APEC*, pp. 1743–1746, 2021, doi: 10.1109/APEC42165.2021.9487348.

[4] P. Podder *et al.*, "Ultra-low loss integrated magnetics platform for high frequency power delivery networks," *CIPS 2020 - 11th Int. Conf. Integr. Power Electron. Syst.*, pp. 81–84, 2020.

[5] X. Xing, N. X. Sun, and B. Chen, "High-bandwidth low-insertion loss solenoid transformers using FeCoB multilayers," *IEEE Trans. Power Electron.*, vol. 28, no. 9, pp. 4395–4401, 2013, doi: 10.1109/TPEL.2012.2233759.

[6] H. Wu, D. S. Gardner, W. Xu, and H. Yu, "Integrated RF on-chip inductors with patterned Co-Zr-Ta-B films," *IEEE Trans. Magn.*, vol. 48, no. 11, pp. 4123–4126, 2012, doi: 10.1109/TMAG.2012.2198448.

[7] D. S. Gardner *et al.*, "Integrated on-chip inductors using magnetic material (invited)," *J. Appl. Phys.*, vol. 103, no. 7, 2008, doi: 10.1063/1.2838012.

[8] C. V Falub *et al.*, "Enhanced permeability dielectric FeCo/Al2O3 multilayer thin films with tailored properties deposited by magnetron sputtering on silicon," *AIP Adv.*, vol. 9, no. 3, p. 35243, Mar. 2019, doi: 10.1063/1.5079477.

[9] L. Cabral, F. H. Aragón, L. Villegas-Lelovsky, M. P. Lima, W. A. A. Macedo, and J. L. F. Da Silva, "Tuning the Magnetic Properties of FeCo Thin Films through the Magnetoelastic Effect Induced by the Au Underlayer Thickness," *ACS Appl. Mater. Interfaces*, vol. 11, no. 1, pp. 1529–1537, 2019, doi: 10.1021/acsami.8b14736.

[10] S. X. Wang, N. X. Sun, M. Yamaguchi, and S. Yabukami, "Properties of a new soft magnetic material ," *Nature*, vol. 407, no. 6801, pp. 150–151, 2000, doi: 10.1038/35025142.

[11] F. Xu, Z. Liao, Q. Huang, C. K. Ong, and S. Li, "Influence of Sputtering Gas Pressure on High-Frequency Soft Magnetic Properties of FeCoN Thin Film," *IEEE Trans. Magn.*, vol. 47, no. 10, pp. 3921–3923, 2011, doi: 10.1109/TMAG.2011.2151834.

[12] T.-J. Hwang, J. Lee, K. H. Kim, and D. H. Kim, "Magnetic properties and high frequency characteristics of FeCoN thin films," *AIP Adv.*, vol. 6, no. 5, 2016, doi: 10.1063/1.4943358.

[13] Z. W. Li, L. Chen, Y. Wu, and C. K. Ong, "Microwave attenuation properties of W-type barium ferrite BaZn2−xCoxFe16O27 composites," *J. Appl. Phys.*, vol. 96, no. 1, pp. 534–539, Jun. 2004, doi: 10.1063/1.1757660.

[14] H. S. Jung, W. D. Doyle, and S. Matsunuma, "Influence of underlayers on the soft properties of high magnetization FeCo films," *J. Appl. Phys.*, vol. 93, no. 10, pp. 6462–6464, May 2003, doi: 10.1063/1.1557653.

[15] P. C. Kuo, S. S. Chang, C. M. Kuo, Y. D. Yao, and H. L. Huang, "Microstructure and magnetic properties of FeCoN thin films," *J. Appl. Phys.*, vol. 83, no. 11, pp. 6643–6645, Jun. 1998, doi: 10.1063/1.367930.

[16] H. Jiang, K. Sin, and Y. Chen, "High Moment Soft FeCoN / NiFe," vol. 41, no. 10, pp. 2896–2898, 2005.

[17] C. R. Sullivan and S. R. Sanders, "Design of microfabricated transformers and inductors for high frequency power conversion," *Ieee Trans. Power Electron.*, vol. 11, no. 2, pp. 228–238, 1996.

[18] J. M. Shin, Y. M. Kim, J. Kim, S. H. Han, and H. J. Kim, "Fabrication of nanocrystalline Fe–Co–Ta–N magnetic films with high saturation magnetization and excellent high-frequency characteristics," *J. Appl. Phys.*, vol. 93, no. 10, pp. 6677–6679, May 2003, doi: 10.1063/1.1556101.

[19] Y. F. Chen, E. Y. Jiang, Z. Q. Li, W. B. Mi, P. Wu, and H. L. Bai, "Structure and magnetic properties of RF sputtered Structure and magnetic properties of RF sputtered Fe – N films," pp. 3–8, 2004, doi: 10.1088/0022-3727/37/10/003.

[20] P. Sharma, H. Kimura, A. Inoue, E. Arenholz, and J. H. Guo, "Temperature and thickness driven spin-reorientation transition in amorphous Co-Fe-Ta-B thin films," *Phys. Rev. B - Condens. Matter Mater. Phys.*, vol. 73, no. 5, pp. 1–4, 2006, doi: 10.1103/PhysRevB.73.052401.

[21] J. M. D. Coey and P. A. I. Smith, "Magnetic nitrides," *J. Magn. Magn. Mater.*, vol. 200, no. 1, pp. 405–424, 1999, doi: https://doi.org/10.1016/S0304-8853(99)00429-1.

[22] N. X. Sun, Q. F. Xiao, and B. York, "Stress, microstructure, and magnetic softness of high saturation magnetization (B s) FeCoN films," in *Journal of Applied Physics*, 2005, vol. 97, no. 10, pp. 1–4. doi: 10.1063/1.1853102.

[23] A. D. C. Viegas *et al.*, "Thickness dependence of the high-frequency magnetic permeability in amorphous Fe73.5 Cu1 Nb3 Si13.5 B9 thin films," *J. Appl. Phys.*, vol. 101, no. 3, 2007, doi: 10.1063/1.2432880.

[24] L. Zhang *et al.*, "High-frequency magnetic properties of [FeCo/FeCo-SiO2]n multilayered films deposited on flexible substrate," *J. Appl. Phys.*, vol. 117, no. 17, p. 17C110, Feb. 2015, doi: 10.1063/1.4907618.

[25] B. Liu *et al.*, "Influence of multiple magnetic phases on the extrinsic damping of FeCo–SiO2 soft magnetic films," *J. Appl. Phys.*, vol. 107, no. 3, p. 33911, Feb. 2010, doi: 10.1063/1.3289588.

[26] R. Das, U. Chaudhuri, and R. Mahendiran, "Microwave Magnetoresistance and Microwave Absorption in Sr2FeMoO6," *ACS Appl. Electron. Mater.*, vol. 3, no. 7, pp. 3072–3078, Jul. 2021, doi: 10.1021/acsaelm.1c00304.

[27] T. Tsutaoka, "Frequency dispersion of complex permeability in Mn–Zn and Ni–Zn spinel ferrites and their composite materials," *J. Appl. Phys.*, vol. 93, no. 5, pp. 2789–2796, Mar. 2003, doi: 10.1063/1.1542651.

[28] C. Kittel, "On the Theory of Ferromagnetic Resonance Absorption," *Phys. Rev.*, vol. 73, no. 2, pp. 155–161, Jan. 1948, doi: 10.1103/PhysRev.73.155.